UC Irvine
UC Irvine Previously Published Works

Title

Two-photon autofluorescence microscopy and spectroscopy of Antarctic fungus: New approach for studying effects of UV-B irradiation

Permalink

https://escholarship.org/uc/item/78x630sw

Journal

Biopolymers, 57(4)

ISSN

1075-4261

Authors

Arcangeli, C
Yu, W
Cannistraro, S
et al.

Publication Date

2000

DOI

10.1002/1097-0282(2000)57:4<218::aid-bip3>3.0.co;2-g

Copyright Information

Peer reviewed

Two-Photon Autofluorescence Microscopy and Spectroscopy of Antarctic Fungus: New Approach for Studying Effects of UV-B Irradiation

C. ARCANGELI,[1][2] W. YU,[3] S. CANNISTRARO,[1][2] E. GRATTON[3]

[1] Unità INFM, Dipartimento di Fisica dell'Università, I-06100 Perugia, Italy

[2] Dipartimento di Scienze Ambientali, Università della Tuscia, I-01100 Viterbo, Italy

[3] Laboratory for Fluorescence Dynamics, Department of Physics, University of Illinois at Urbana–Champaign, Urbana, Illinois 61801

ABSTRACT: We combined two-photon fluorescence microscopy and spectroscopy to provide functional images of UV-B (280–315 nm) induced stress on an Antarctic fungus. Two-photon excitation microscopy was used to characterize the distribution of autofluorescence inside the spore and the hyphae of the fungus. The imaging analysis clearly shows that the autofluorescence response of spores is higher than that of hyphae. The imaging analysis at different depths shows that, strikingly enough, the spore autofluorescence originates from the cell wall and membrane fluorophores. The spectroscopic results show moreover that the fluorescence spectra of spores are redshifted upon UV-B irradiation. Tentative identification of the chromophores involved in the autofluorescence response and their biological relevance are also discussed on the basis of a previous steady-state fluorescence spectroscopic study performed on both whole spore suspension and organic-soluble extracts. © 2000 John Wiley & Sons, Inc. Biopolymers (Biospectroscopy) 57: 218–225, 2000

Keywords: two-photon autofluorescence; UV-B effects; Antarctic fungus

INTRODUCTION

Autofluorescence spectroscopy has proved to be a very sensitive and useful tool in understanding cell behavior. Recent literature shows a remarkable growth of interest in the autofluorescence of whole cells and tissues. Efforts have been made to exploit the blue-green emission for stress detection in plant cells[1,2] and for physiological and clinical diagnostic investigation of tumors.[3–6]

We recently investigated the steady-state fluorescence spectroscopic properties of whole cells of *Arthrobotrys ferox*,[7] which is a terrestrial fungus (hyphomycete) isolated from moss samples in Wood Bay (Victoria Land, Continental Antarctica).[8] *A. ferox* produces interwoven aerial hyphae and reproduces by means of septate spores, which are naturally dispersed in the surrounding environment and therefore may be subjected to environmental stress. We were interested in the emerging issues concerning the UV radiation stress due to the depletion of stratospheric ozone occurring in Antarctica[9] and also in the perspective of the potential use of *A. ferox* as a bioindica-

tor. Studies were carried out on Antarctic organisms to study whether those organisms may develop defenses to tolerate the increased UV radiation level.[10–12] Many Antarctic invertebrate and algal species display some degree of natural biochemical protection against UV exposure, which is possibly connected to the presence of photoprotective carotenoids and mycosporine-like amino acids (MAAs).[10–12] Conversely, little information is available on the potential photoprotective role played by carotenoids and other pigments in fungi. However, the strong pigmentation of the typical lichen genera of Antarctica is interpreted as a response to the frequently high irradiance levels and perhaps as an effective protection against UV irradiation.[13]

Previous steady-state fluorescence spectroscopic characterization of whole spores suggested the involvement of several chromophores in the autofluorescence response, such as reduced nicotinamide adenine dinucleotide (phosphate) [NAD(P)H] and flavoproteins whose fluorescence was substantially enhanced under UV irradiation.[7] On the basis of experiments performed on organic-soluble fluorophores extracted from spores, we suggested that the UV exposure was also responsible for accumulation of age pigments and photodestruction of carotenoids.[7]

However, a number of problems are encountered when fluorescence spectroscopy is applied on spore suspensions that are due to the complexity of the system. The deconvolution of whole cell spectra to yield the nature and the concentration of chromophores involved in the physiological process of interest proved difficult because of the highly scattering and absorbing characters of cells and tissues.[6,14–16]

We revisit the problem by exploiting the novel capabilities offered by the combination of the two-photon excited autofluorescence microscopy and spectroscopy to better understand the nature and the spatial localization of chromophores and to study their autofluorescence changes under enhanced UV-B (280–315 nm) irradiation.

Two-photon excitation arises from the simultaneous absorption of two photons.[17] In particular, two-red photon absorption causes a transition to an excited electronic state normally reached by absorption in the UV. Each photon provides half the energy required for excitation. Because the probability of two-photon absorption depends on the virtually simultaneous colocalization of both photons within the absorption cross section of the fluorophores, the number of excitations is propor-

tional to the square of the instantaneous intensity. In practice, the high photon densities required for two-photon absorption are achieved by focusing a high peak power laser on a diffraction-limited spot through a high numerical aperture objective. Hence, the excitation is limited to the focal volume, even though the red light is present throughout the sample. This inherent localization provides depth discrimination and background elimination equivalent to confocal microscopy without requiring a confocal spatial filter, whose absence enhances fluorescence collection efficiency.[18,19] Further, the confinement of excitation to the focal volume also greatly reduces photobleaching and photodamage. Another advantage of the two-photon excitation is the relative transparency of biological specimens to red light, allowing deeper sectioning, because absorbance and scattering are both reduced.[18,19]

Our results clearly show that the hyphae autofluorescence is much less marked than that of the spore. The imaging analysis at different depths and the spectroscopic results reveal the involvement in the spore autofluorescence of wall–membrane pigments whose spectra change substantially after UV-B (280–315 nm) irradiation.

MATERIALS AND METHODS

Preparation of Biological Samples

Pure cultures of *A. ferox* strain CBS137.91 were grown on Czapek-agar (Difco) and maintained at room temperature. They were grown under sunlight and shielded from UV light by means of a UV opaque glass until the occurrence of sporulation (ca. 20 days). A part of the colony, which was grown on a cellophane dish to facilitate its harvesting and to avoid disturbances from the substrate components in the measurements, was placed on the microscope slide. Then the coverslip was mounted on the microscope slide.

Two-Photon Scanning Microscope

The two-photon scanning microscope was previously described and the experimental setup used in our experiments is the same as that shown by So et al.[20,21] A femtosecond Ti-sapphire laser (Mira 900; Coherent, Palo Alto, CA) tuned to 770 nm was used as the light source. The laser light was guided by a galvanometer-driven *x–y* scanner

(Cambridge Technology, Watertown, MA) to achieve beam scanning in both the x and y directions. The scan parameters were chosen such that 256×256 pixel images were generated with a pixel residence time of 320 μs corresponding to a frame rate of about 26 s. The laser power entering the microscope was adjusted to 35 mW via a Glan–Thompson polarizer. The sample receives about one-tenth of the incident power. The vertical position of the objective can be adjusted by a stepper motor coupled to the manual micropositioning knob of the microscope. A linear variable differential transformer (Schaevitz Engineering, Cadmen, NJ) monitors the z position. A single-board computer (8052 microprocessor, Iota System, Inc., Incline Village, NV) actively reads the position of the linear variable differential transformer and controls the motion of the stepper motor. An accuracy of 20 nm in the z position can be achieved. The excitation light enters the Zeiss Axiovert 35 microscope (Zeiss, Thornwood, NY) via a modified epiluminescence light path. The light is reflected by the dichroic mirror to the Zeiss 40× Plan-Fluor (1.3 N.A., oil) objective. The objective produces a lateral displacement of 0.25 μm per pixel, corresponding to an image size of 64 μm. The actual measuring focal volume is defined by an ellipsoid about 0.3 μm in diameter and 1 μm in length. The fluorescence signal (from 400 to 600 nm) is collected by the same objective, transmitted through the dichroic mirror and the barrier filter (3 mm BG-39, CVI Laser, CA), and refocused on the detector. A miniature photomultiplier (R5600-P, Hamamatsu, Bridgewater, NJ) amplified by an AD6 discriminator (Pacific, Concord, CA) was used for light detection in the photon counting mode. The counts were acquired by a home-built card in a PC computer.

Measurement of Fluorescence Emission Spectrum in Microscope

We performed spectral measurements of the *A. ferox* spores at selected points. A monochromator was inserted between the microscope and the photomultiplier tube. The wavelength resolution was set by the monochromator slit to 8 nm. Scan frames of the same colony focal field were acquired at a 5-nm emission wavelength step. The scan parameters were chosen such that 256×256 pixel images were generated with a pixel residence time of 1.6 ms corresponding to a frame rate of about 130 s.

The spectra were obtained by choosing a cell area of interest (5×5 pixels corresponding to an area of about 1.6 μm^2) for each emission wavelength frame and by averaging over all intensity values of that area.

Irradiation Method

The sample was irradiated by means of an XBO (300-W xenon) lamp. In order to use the light emitted in the UV-B, UV-A, and visible range, a Schott longpass filter WG280 ($T = 50\%$ at 280 nm), which cuts off the UV-C range, was used. For simplicity, the irradiation condition is referred to as UV-B irradiation. In order to remove IR radiation emitted from the lamp, a quartz water-filled cell placed between the lamp and the sample was used.

The samples were irradiated with an intensity of 10.5 mW cm^{-2} up to 60 min (2.0×10^{-2} m irradiation spot diameter, 37.8 J cm^{-2} radiant exposure) and examined immediately at the microscope after irradiation.

RESULTS AND DISCUSSION

Two-Photon Imaging of *A. ferox*

We analyzed the autofluorescence images from 10 different *A. ferox* colonies. Although we observed some differences in the intensity values, according to the analyzed section location within the cells, the autofluorescence distribution within the cells was almost the same. In particular, the ratio between the autofluorescence intensity due to the cell border region and that due to the cell cytoplasmic region turned out to be 4.0 ± 0.8.

Figure 1 shows typical autofluorescence images (from 400 to 600 nm) of an *A. ferox* colony. *A. ferox* produces interwoven aerial hyphae and ovoid septate spores that are slightly constricted in the septum, which is usually in the middle of the cell. The color scale in the figure indicates fluorescence intensity. In Figure 1(A) we can distinguish spores from hyphae and we observe that the autofluorescence intensity of hyphae is less marked than that of spores. For this reason we focused our attention only on the autofluorescence response of the *A. ferox* spores. The most striking feature is that the brighter fluorescent regions correspond to patches on the spore borders. In addition, some morphological structures such as the septum [see arrows shown in Fig. 1(B)], which is a constriction of the membrane
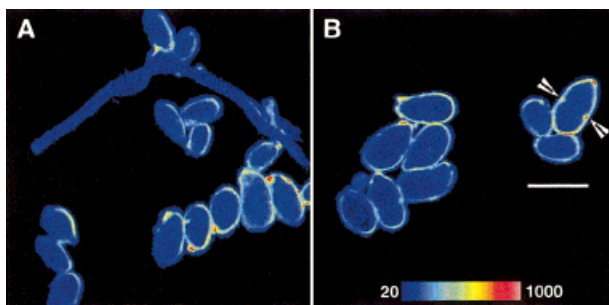
Figure 1. Representative autofluorescence images of (A) *Arthrobotrys ferox* colony and (B) spores. The spectral range for detection of microscopic images is 400–600 nm. Scale bar = 12.5 μm. Each images is 64 × 64 μm. The color scale indicates the fluorescence intensity.

and wall cell, show high values of autofluorescence.

To better assess the origin of the spore autofluorescence, sectioning along the z axis was performed. Spores of 12–14 μm diameter were imaged at steps of 2 μm along the z axes. A representative montage of images from a complete stack is shown in Figure 2. At about 4–6 μm [see Fig. 2(C,D)] we observe that the spore autofluorescence (400–600 nm spectral range) originates from fluorescence-enriched domains on

the cell border. A weaker fluorescent signal from the cytoplasm is also observed.

Generally, the autofluorescence of mammalian cells originates from the organelles inside the cytoplasm. Indeed, Piston et al.[22] observed that the two-photon excited autofluorescence in the epithelial and endothelial cells of rabbit corneas arises from the cytoplasmic region of the cells. In a similar way, the strongest fluorescence signal of Chinese hamster ovary cells was found to arise from cytoplasmic mitochondria.[23] Further, Masters et al.[24] used multiphoton excitation fluorescence microscopy to observe punctuated fluorescence within the cytoplasm of human skin cells. They related these fluorescent organelles to mitochondria with a high concentration of NAD(P)H.

In our cellular system we observed a bright fluorescent signal due to border fluorophores that obscures that due to weaker cytoplasmic chromophores. Indeed, in Figure 3 we focused our attention on the cytoplasmic region [Fig. 3(B)] by increasing the image contrast. We can observe that the cell nuclei appear dark because of the absence of fluorescence and that only a weak fluorescent signal (about 4 times less than that due to the border region) from cytoplasmic organelles is observed. From the cell morphology the fluorescence-enriched domains observed in *A. ferox*
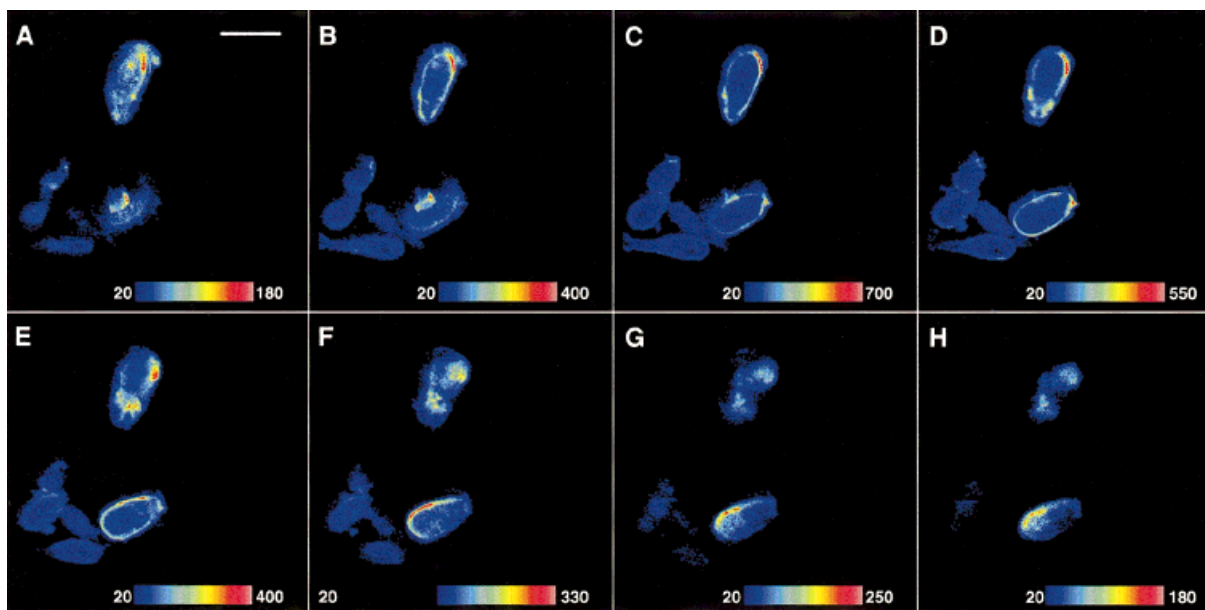

Figure 2. A representative montage of 2-dimensional sections of *Arthrobotrys ferox* spores at successive depths. The depth separation of each image is 2 μm. The spectral range for detection of microscopic images is 400–600 nm. Scale bar = 12.5 μm. The color scale indicates the fluorescence intensity.
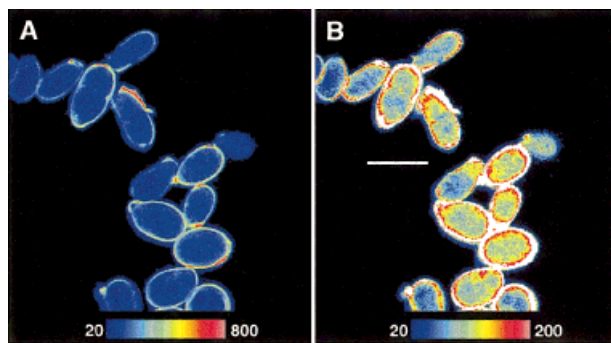
Figure 3. (A) An autofluorescence image of *Arthrobotrys ferox* spores. (B) The same image but seen through a different chromatic intensity scale to reveal the cytoplasmic autofluorescence. The spectral range for detection of microscopic images is 400–600 nm. Scale bar = 12.5 μm. The color scale indicates the fluorescence intensity.

spores could belong to membrane and wall structures.

In Figure 4 we show the effect of UV-B (280–315 nm) irradiation on autofluorescence intensity. The autofluorescence responses (from 400 to 600 nm) of the control and UV-B irradiated samples are shown in Figure 4(A,B), respectively. Although the two autofluorescence images are not related to the same focal field, a detailed analysis on several UV-B irradiated samples undoubtedly showed uniform responses. There are no substantial changes concerning the distribution of autofluorescence on the border of spores after UV-B irradiation. However, one should note that punctuated fluorescence within the cytoplasm of UV-B irradiated spores was also observed.

Emission Spectroscopy at Selected Points on *A. ferox*: Effect of UV-B

While microscopic imaging analysis allows us to localize the distribution of fluorophores in the autofluorescence response, spectroscopic analysis may help to assess the molecular nature of the involved fluorophores and the UV-B induced changes on their fluorescence response.

The spectroscopic data were obtained at selected points on the *A. ferox* spores using a 770-nm excitation wavelength corresponding to a one-photon excitation wavelength of about 385 nm. Several emission spectra at different and selected points on the border region and on the cytoplasm of spores were recorded, revealing similar responses.

Figure 5 shows typical emission spectra obtained at selected points on the border region of *A. ferox* spores before and after UV-B irradiation. The whole emission band is wide, covering a region from 400 to 500 nm. In the control spore spectrum a peak at about 445 nm is seen. After UV-B (280–315 nm) irradiation a redshifted spectrum with a maximum at 455 nm and a shoulder at about 475 nm is observed.

For comparison, the typical emission spectrum obtained at selected points on the spore cytoplasm before and after UV-B (280–315 nm) irradiation is shown in the inset of Figure 5. The emission response from the cytoplasm (inset of Fig. 5) is much weaker than that observed for wall–membrane structures (Fig. 5), which is also according to the imaging results (see Fig. 3). We also observed that the cytoplasmic autofluorescence showed an emission behavior similar to that obtained from the border region. Indeed, a wide emission band from 400 to 500 nm with a peak at about 440 nm and a shoulder at about 465 nm can be observed for the cytoplasmic emission spectrum of the control sample. A redshifted spectrum with a maximum at 455 nm and a shoulder at about 475 nm is observed after UV-B irradiation.

On the basis of the spatial localization within the cell, the nature of the chromophores involved in the autofluorescence response could be assessed in principle. In this respect, even if some similarities between the two emission spectra exist, the emission response from the cytoplasm (inset of Fig. 5) seems to be consistent with that of NAD(P)H and flavin molecules. Because NAD(P)H and flavin molecules apparently are not localized on the wall and membrane structures, the stron-
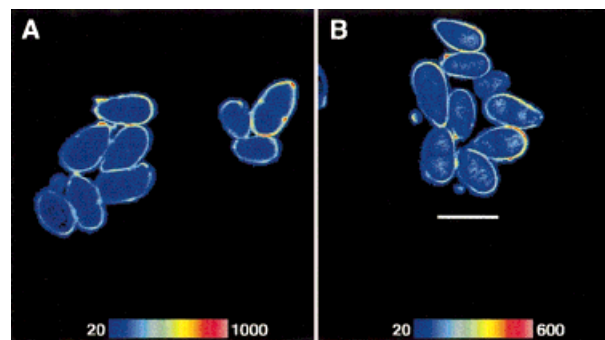

Figure 4. Autofluorescence images of (A) control and (B) UV-B irradiated *Arthrobotrys ferox* spores. The spectral range for detection of microscopic images is 400–600 nm. Scale bar = 12.5 μm. The color scale indicates the fluorescence intensity.
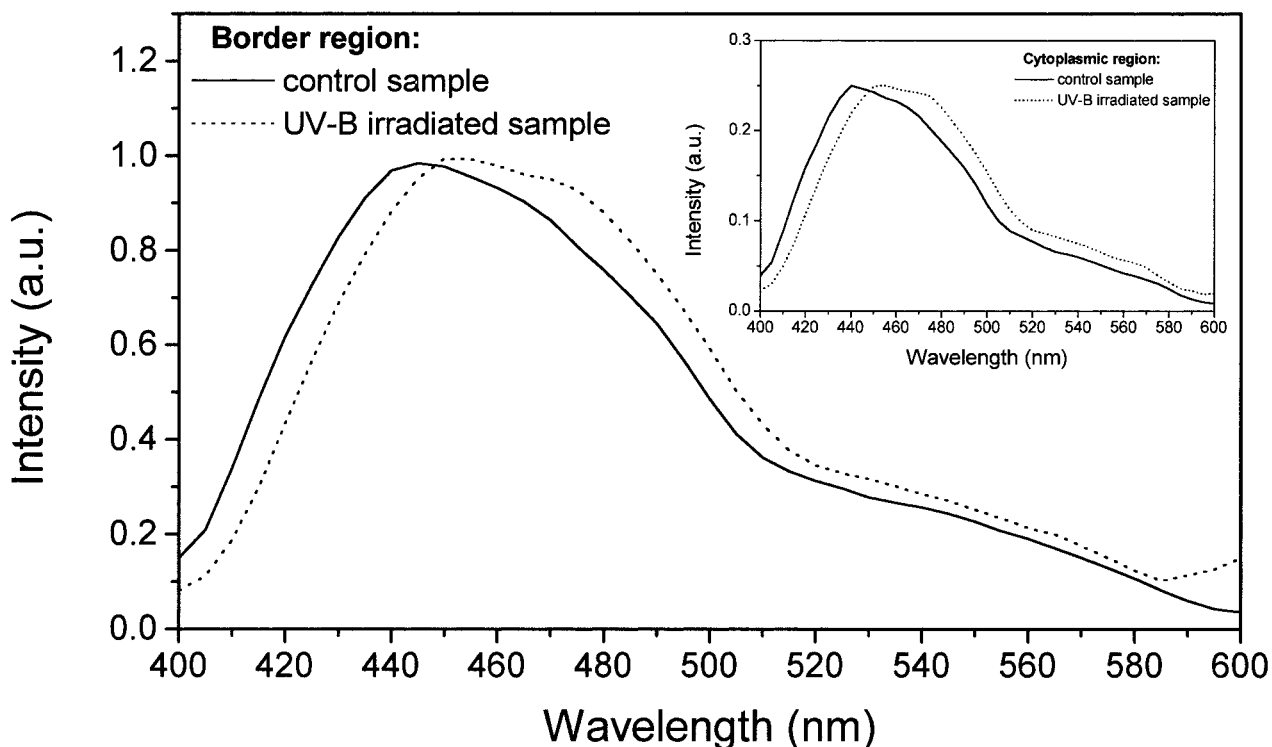
Figure 5. Emission spectra of (—) control and (- - -) the UV-B irradiated border region of *Arthrobotrys ferox* spores at a 770-nm excitation wavelength. Inset: Emission spectra of (—) control and (- - -) the UV-B irradiated cytoplasmic region of *A. ferox* spores at a 770-nm excitation wavelength. The spectra are corrected for the BG39 filter transmittance spectrum and the intensity is given in arbitrary units.

gest fluorescence signal from the border region (Fig. 5) should instead be related to other wall–membrane pigments.

The redshifted spectra observed for both cytoplamic and border structures after UV-B irradiation (Fig. 5) are consistent with those obtained by means of steady-state spectroscopy on spore suspensions that showed a marked redshift after UV irradiation.[7] In this respect, we should take into consideration that a marked redshift might be due to light scattering and reabsorption phenomena occurring in spore suspensions and more generally in cells and tissues.[6,14–16] In particular, it has been found that the intrinsic presence of multiple scatterers in a cell greatly enhanced the random walk of the emitted photons from cells, giving rise to redshifted spectra with respect to the intrinsic fluorescence emission.[16] Such a phenomenon is known to be drastically reduced by using two-photon excitation.[18,19] Indeed, with two-photon excitation the redshift appears less marked but still significant; therefore, it appears reasonable to attribute this spectral shift to the

UV irradiation. In addition, we remark that such an induced UV irradiation spectral shift should be related only to the UV-B part (280–315 nm) of the xenon lamp spectrum used for the irradiation method. Indeed, as previously assessed, no appreciable changes in the spore emission signals are observed if the lamp radiations with $\lambda < 320$ nm are cut off by means of a longpass filter.[7] In our previous work[7] we suggested that the UV-induced red shift was mainly due to differences in the environment and concentration of the electron–proton redox molecules, such as NAD(P)H and flavoproteins, according to the literature.[1,3] On the basis of a spectroscopic investigation on organic-soluble extracts from spores, we also suggested that the UV exposure was responsible for an accumulation of pigments connected to induced senescence processes and photodestruction of carotenoids.[7]

On the basis of the two-photon microscopic and spectroscopic results, which showed the spatial localization of the main chromophores on the border region of the spores, we should reconsider the

previous attribution. As already mentioned, because NAD(P)H and flavin molecules apparently are not localized on the wall and membrane structures, their involvement in the brighter fluorescent signal of spores should be ruled out. Therefore, we focused our attention on those pigments that are known to be incorporated into fungal cell walls. To the best of our knowledge, the pigment composition of *A. ferox* is still unknown. Gams and Boekhout[25] used transmission electron microscopy to identify different wall layers of pigmented elements in dematiaceous hyphomycetes without providing with any information about the nature of the pigment composition. On the other hand, Valadon and Cooke[26] used chromatographic methods to isolate and characterize carotenoid pigments, such as β- and γ-carotene, torulene, and neurosporoxanthin in *A. oligospora*, a species very similar to *A. ferox*, and suggested the use of these pigments as additional taxonomic characteristics of fungi.[27] Moreover, experimental evidence of the presence of carotenoid pigments on the wall–membrane regions of *A. ferox* spores was recently obtained by Raman microspectroscopic spectra.[28] Even if some carotenoid fluorescence is reported in the literature,[29–31] it is commonly believed that carotenoids display weak fluorescence. Therefore, the wall–membrane autofluorescence response in *A. ferox* should involve other strong fluorescing pigments, such as fungal anthraquinone pigments (e.g., chrysogenin, emodin, asperthecin, tajixanthone and versicolorone), and mycotoxins (e.g., ochratoxin A and aflatoxin).[32–36] In addition, age pigments and mycosporines were shown to be involved in the fluorescence spectra of *A. ferox* spores.[7]

On such grounds, the autofluorescence emission of *A. ferox* spores seem to be constituted of a complex signal that is probably due to overlapping responses of a number of wall–membrane pigments. On the basis of these considerations, the changes in the two-photon emission spectra after UV-B (280–315 nm) irradiation could be attributed to accumulation of age pigments and to possible damage or modification occurring to the above-mentioned wall–membrane pigments.

In this respect it is interesting to note that colorless (hyaline) conidia from a variety of fungi are known to be more sensitive to UV irradiation.[37] In addition, antraquinones and MAAs are both believed to play a possible role in protecting from UV light and/or acting as a photoreceptor on the basis of their strong absorbance between 200 and 300 nm.[33,38–41] In our case, the onset of a weak cytoplasmic fluorescence response upon UV irradiation, which is possibly due to electron–proton redox molecules [see Fig. 4(B)], might be subsequent to UV-induced phodestruction of wall–membrane pigments.

A definitive attribution of fluorophores involved in the wall–membrane autofluorescence response requires further biochemical and spectroscopic investigations because there is a lack of information concerning the pigment composition in the *A. ferox* fungus.

CONCLUSIONS

Two-photon microscopy and spectroscopy proved to be a sensitive and useful tool to assess the origin of spore autofluorescence and to detect the UV-B induced spectral changes.

Our new results represent a substantial improvement over our previous attribution of autofluorescence response in this fungus. In particular, on the basis of the microscopic images we infer that the spore autofluorescence arises from cell wall–membrane fluorophores. The recording of emission spectra further enabled some characterization of the source of the spore autofluorescence. The two-photon emission spectra after UV-B irradiation were redshifted according to previous observations on spore suspension.[7] However, the early attribution of redox molecules, such as NAD(P)H and flavoprotein molecules, as the main fluorescence source is now reconsidered on the basis of spatial localization of cromophores assessed by two-photon microscopy. Wall–membrane pigments and age pigments could provide the main contribution to the spore fluorescence signal. The UV-B induced changes in the spore emission spectra could be due to possible accumulation of age pigments and/or possible damage or modification occurring to the molecular structure of wall–membrane pigments. In this respect, additional spectroscopic and biochemical investigations are in progress to provide a definitive identification of the pigments involved in the wall–membrane autofluorescence response.

The specificity and reproducibility of the autofluorescence response, as well as the spectral changes observed after UV-B irradiation, establish two-photon microscopy and spectroscopy as a sensitive and nondestructive approach for studying cell behavior.

REFERENCES

1. Goulas, Y.; Moya, I.; Schmuck, G. Photosynth Res 1990, 25, 299–307.
2. Sgarbossa, A.; Lucia, S.; Lenci, F.; Gioffre', D.; Ghetti, F.; Checcucci, G. J Photochem Photobiol B Biol 1995, 27, 243–249.
3. König, K.; Schneckenburger, H. J Fluoresc 1994, 4, 17–40.
4. König, K.; Liu, Y.; Sonek, G. J.; Berns, M. W.; Tromberg, B. J. Photochem Photobiol 1995, 62, 830–835.
5. Anidjad, M.; Cussenot, O.; Blais, J.; Bourdon, O.; Avrillier, S.; Ettori, D.; Villette, J.-M.; Fiet, J.; Teillac, P.; Le Duc, A. J Urol 1996, 155, 1771–1774.
6. Richards-Kortum, R.; Sevick-Muraca, E. Annu Rev Phys Chem 1996, 47, 555–606.
7. Arcangeli, C.; Zucconi, L.; Onofri, S.; Cannistraro, S. J Photochem Photobiol B Biol 1997, 39, 258–264.
8. Onofri, S.; Tosi, S. Mycotaxon 1992, 64, 445–451.
9. Frederick, J. E.; Snell, H. E. Science 1988, 241, 438–440.
10. Smith, R. C.; Prezelin, B. B.; Baker, K. S.; Bidigare, R. R.; Boucher, N. P.; Coley, T.; Karentz, D.; MacIntyre, S.; Matlick, H. A.; Menzies, D.; Ondrusek, M.; Wan, Z.; Waters, K. J. Science 1992, 255, 952–959.
11. Karentz, D.; Bosch, I.; Dunlap, W. C. Antarctic J US 1992, 27, 121–122.
12. Post, A.; Larkum, A. D. W. Aquat Bot 1993, 45, 231–243.
13. Kappen, L. In Antarctic Microbiology; Friedmann, E. I., Ed.; Wiley–Liss: New York, 1993; pp 433–490.
14. Das, B. B.; Yoo, K. M.; Liu, F.; Cleary, J.; Prudente, R.; Celmer, E.; Alfano, R. R. Appl Opt 1993, 32, 549–553.
15. Durkin, A. J.; Jaikumar, S.; Ramanujam, N.; Richards-Kortum, R. Appl Opt 1994, 33, 414–423.
16. Ahmed, S. A.; Zang, Z.-W.; Yoo, K. M.; Ali, M. A.; Alfano, R. R. Appl Opt 1994, 33, 2746–2750.
17. Denk, W.; Strickler, J. H.; Webb, W. W. Science 1990, 248, 73–76.
18. Denk, W.; Piston, D. W.; Webb, W. W. In Handbook of Biological Confocal Microscopy; Pawley, J. B., Ed.; Plenum: New York, 1995; pp 445–458.
19. Sandison, D. R.; Piston, D. W.; Webb, W. W. In Three-Dimensional Confocal Microscopy: Volume Investigation of Biological Systems; Stevens, J. K., Mills, L. R., Trogadis, J. E., Eds.; Academic: New York, 1994; pp 29–45.
20. So, P. T. C.; French, T.; Yu, W. M.; Berland, K. M.; Dong, C. Y.; Gratton, E. Bioimaging 1995, 3, 49–63.
21. So, P. T. C.; French, T.; Yu, W. M.; Berland, K. M.; Dong, C. Y.; Gratton, E. In Fluorescence Imaging Spectroscopy and Microscopy, Chemical Analysis Series; Wang, X. F., Herman, B., Eds.; Wiley: New York, 1996; Vol. 137, pp 351–374.
22. Piston, D. W.; Masters, B. R.; Webb, W. W. J Microsc 1995, 178, 20–27.
23. König, K.; So, P. T. C.; Mantulin, W. W.; Tromberg, B. J.; Gratton, E. J Microsc 1996, 183, 197–204.
24. Masters, B. R.; So, P. T. C.; Gratton, E. Biophys J 1997, 72, 2405–2412.
25. Gams, W.; Boekhout, T. Proc Ind Acad Sci (Plant Sci) 1985, 94, 273–280.
26. Valadon, L. R. G.; Cooke, R. C. Phytochemistry 1963, 2, 103–105.
27. Valadon, L. R. G. Trans Br Mycol Soc 1976, 67, 1–15.
28. Arcangeli, C.; Cannistraro, S. Biospectroscopy 2000, 57, 179–186.
29. Blankenhorn, D. H.; Braunstein, H. J Clin Invest 1958, 37, 160–165.
30. Deckelbaum, L. J.; Lam, J. K.; Cabin, H. S.; Soni Clubb, K.; Long, M. B. Lasers Surg Med 1987, 7, 330–335.
31. Chappelle, E. W.; McMurtrey III, J. E.; Kim, M. S. Remote Sens Environ 1991, 36, 213–218.
32. Gill, M.; Steglich, W. In Progress in the Chemistry of Organic Natural Products; Herz, W., Grisebach, H., Kirby, G. W., Tamm, C. H., Eds.; Springer–Verlag: New York, 1987; pp 1–137.
33. Trinci, A. P.; Banbury, G. H. Trans Br Mycol Soc 1969, 52, 73–86.
34. Wolf, F. T.; Kim, Y. T.; Jones, A. Physiol Pl 1960, 13, 621–627.
35. Frohlich, A. A.; Marquardt, R. R.; Bernatsky, A. J Off Anal Chem 1988, 71, 949–953.
36. Goldblatt, L. A. Aflatoxin. Scientific Background, Control and Implication; Academic: New York, 1969.
37. Wheeler, M. H.; Bell, A. A. Curr Top Med Mycol 1988, 2, 338–387.
38. Brown, D. W.; Salvo, J. J. Appl Environ Microbiol 1991, 60, 979–983.
39. Arpin, N.; Bouillant, M. L. In The Fungal Spore, Morphogenetic Controls; Turian, G., Hohl, H. R., Eds.; Academic: London, 1981; pp 435–454.
40. Sivalingam, P. M.; Ikawa, T.; Nisizawa, K. Bot Mar 1976, 19, 1–7.
41. Karentz, D.; McEuen, F. S.; Land, M. C.; Dunlap, W. C. Mar Biol 1991, 108, 157–166.